The new facial tripod ligand 3,3-bis(1-methylimidazol-2-yl)propionic acid and carbonyl complexes thereof containing manganese and rhenium

Liv Peters, Eike Hübner, Nicolai Burzlaff *

Fachbereich Chemie, Universität Konstanz, Universitätsstraße 10, Fach M728, D-78457 Konstanz, Germany

Abstract

The new facially coordinating tripod ligand 3,3-bis(1-methylimidazol-2-yl)propionate (bmip) has been studied. A synthetic route to sodium 3,3-bis(1-methylimidazol-2-yl)propionate (Na[bmip], **2a**) and its hydrochloride (Hbmip · 2HCl, **2b**) is reported. The electronic properties of Hbmip were calculated by DFT methods and are compared to those of structurally similar bis(pyrazol-1-yl)acetic acids. The ligand was applied in the synthesis of the two tricarbonyl complexes [Re(bmip)(CO)$_3$] (**3**) and [Mn(bmip)(CO)$_3$] (**4**). Methyl 3,3-bis(1-methylimidazol-2-yl)propionate (bmipme) (**1**), which is the precursor of Hbmip, and the complexes [Re(bmip)(CO)$_3$] (**3**) and [Mn(bmip)(CO)$_3$] (**4**) were characterised by single crystal X-ray analysis.
© 2004 Elsevier B.V. All rights reserved.

1. Introduction

During the last decade facially coordinating tripod ligands such as hydridotris(pyrazol-1-yl)borates (Tp, Tp^{Me_2}) and bis(pyrazol-1-yl)acetic acids (bpza, bdmpza) have become widely used in the fields of both coordination chemistry and bioinorganic chemistry [1–4]. In coordination chemistry these ligands are often considered as equivalents to C$_5$H$_5^-$ (Cp) or C$_5$Me$_5^-$ (Cp*) (Fig 1). In bioinorganic chemistry these ligands have been applied in model complexes for the active sites of metalloenzymes containing the so-called 2-His-1-carboxylate motif. This binding motif, where a metal ion (e.g., Fe^{2+}, Zn^{2+}) is bound by two histidine residues and a glutamate or aspartate residue, is common to several classes of enzymes, such as mononuclear non-heme iron(II) enzymes (e.g., TauD, IPNS, CAS) and gluzincins (e.g., thermolysin) [3,4]. Inspired by the 2-His-1-carboxylate motif our interest focused on the development of a new facially coordinating tripod ligand which resembles the electronic properties of this binding motif more closely. A possible way of achieving this is the use of imidazolyl instead of pyrazolyl residues. Such a ligand will be closely related to bdmpza and bpza and hence also to Tp and Tp^{Me_2}. Therefore, it will be of use not only in bioinorganic chemistry, but also in coordination chemistry. So far research has focused on 3,3-bis(imidazol-2-yl)propionic acid (Hbip) and derivatives of it [5–7].

Here, we report on (a) DFT calculations comparing 1,2-dimethylimidazole with 1-methylpyrazole, (b) the synthesis of the new ligand sodium 3,3-bis(1-methylimidazol-2-yl)propionate (Na[bmip]) and (c) the preparation of complexes [M(bmip)(CO)$_3$] with M = Re, Mn (see Fig. 1).

* Corresponding author. Tel.: +49 7531/88 2053; fax: +49 7531/88 3136.

E-mail address: nicolai@chemie.uni-konstanz.de (N. Burzlaff).
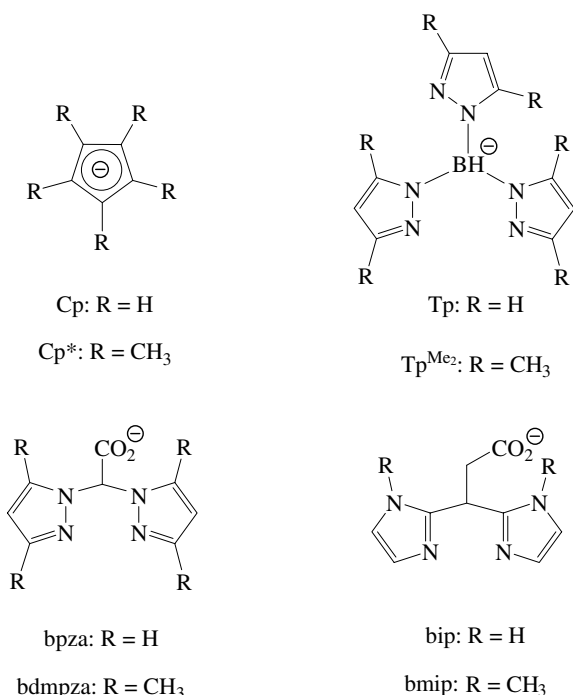
Fig. 1. The ligands Cp, Cp*, Tp, Tp^{Me_2}, bpza, bdmpza, bip and bmip.

Scheme 1. Synthesis of bmipme (**1**), Na[bmip] (**2a**) and Hbmip · 2HCl (**2b**).

2. Results and discussion

2.1. DFT calculations

For a comparison of the coordination properties of histidine, pyrazol-1-yl and 1-methylimidazol-2-yl ligands DFT calculations were performed on histidine, 1-methylpyrazole and 1,2-dimethylimidazole. The frontier orbitals of 1-methylpyrazole are assumed to be comparable to those of the pyrazol-1-yl groups in bis(pyrazol-1-yl)acetato ligands, and those of 1,2-dimethylimidazole should be closely related to the 1-methylimidazol-2-yl groups in a bis(1-methylimidazol-2-yl)acetato or a 3,3-bis(1-methylimidazol-2-yl)propionato ligand. The contour plots of the corresponding frontier orbitals are shown in Fig. 2.

As described by Holm et al. [8] the σ- and π-binding ability of histidine is determined by its frontier orbitals. Their calculations show that histidine is not only a σ- and π-donor but a π-acceptor ligand as well. Our calculated plots of the histidine frontier orbitals correspond well with these findings. Generally speaking 1-methylpyrazole shows binding abilities and orbital energies similar to those of histidine, but there are some remarkable differences: The HOMO − 2 of 1-methylpyrazole is capable of a σ-donor bond, whereas in histidine the HOMO − 2 forms a π-donor. The HOMO − 1 of 1-methylpyrazole may form a π-donor bond. In histidine however the HOMO − 1 is utilised for a σ-donor bond. The HOMO of histidine probably does not play an important role in binding to the metal centre, since the

orbital coefficient at the nitrogen atom is very small. In contrast, the HOMO of 1-methylpyrazole is also capable of a π-donor bond. Additionally, both the LUMO + 1 of histidine and the LUMO of 1-methylpyrazole form π-acceptors. The LUMO of 1-methylpyrazole is lower in energy, whereas the LUMO + 1 of histidine is slightly higher in energy [9]. Furthermore, all orbitals of 1-methylpyrazole have larger coefficients at the coordinating nitrogen atom than those of the corresponding orbitals of histidine. Consequently, pyrazol-1-yl ligands might be stronger σ-donors, π-donors and especially π-acceptors than histidine itself. In contrast, 1,2-dimethylimidazole resembles histidine more closely not only in its orbital energies, but also in terms of orbital coefficients at the coordinating nitrogen atom. The HOMO − 2 is capable of forming a π-donor bond, the HOMO − 1 can be utilised for a σ-donor bond, and the orbital coefficient of the nitrogen atom in the HOMO is very small, similar to histidine. The LUMO of 1,2-dimethylimidazole is slightly higher in energy and may be involved in a π-acceptor bond. In short, the DFT calculations indicate that both 1-methylimidazol-2-yl and pyrazol-1-yl ligands possess, similar to histidine, σ-donor, π-donor and π-acceptor properties. But a 3,3-bis(1-methylimidazol-2-yl)propionato ligand probably resembles the overall binding properties of histidine closer than a bis(pyrazol-1-yl)acetato ligand.

2.2. Synthesis of 3,3-bis(1-methylimidazol-2-yl)-propionic acid

For a direct comparison to bis(pyrazol-1-yl)acetic acids (Hbdmpza, Hbpza) it would have been desirable to synthesise 3,3-bis(1-methylimidazol-2-yl)acetic acid. But during the synthesis of this ligand we found, that it decarboxylates rather easily. Therefore, we concentrated on the development of 3,3-bis(1-methylimidazol-2-yl)-propionic acid, which is more stable. 3,3-bis(1-methylimidazol-2-yl)propionic acid was synthesised in two steps
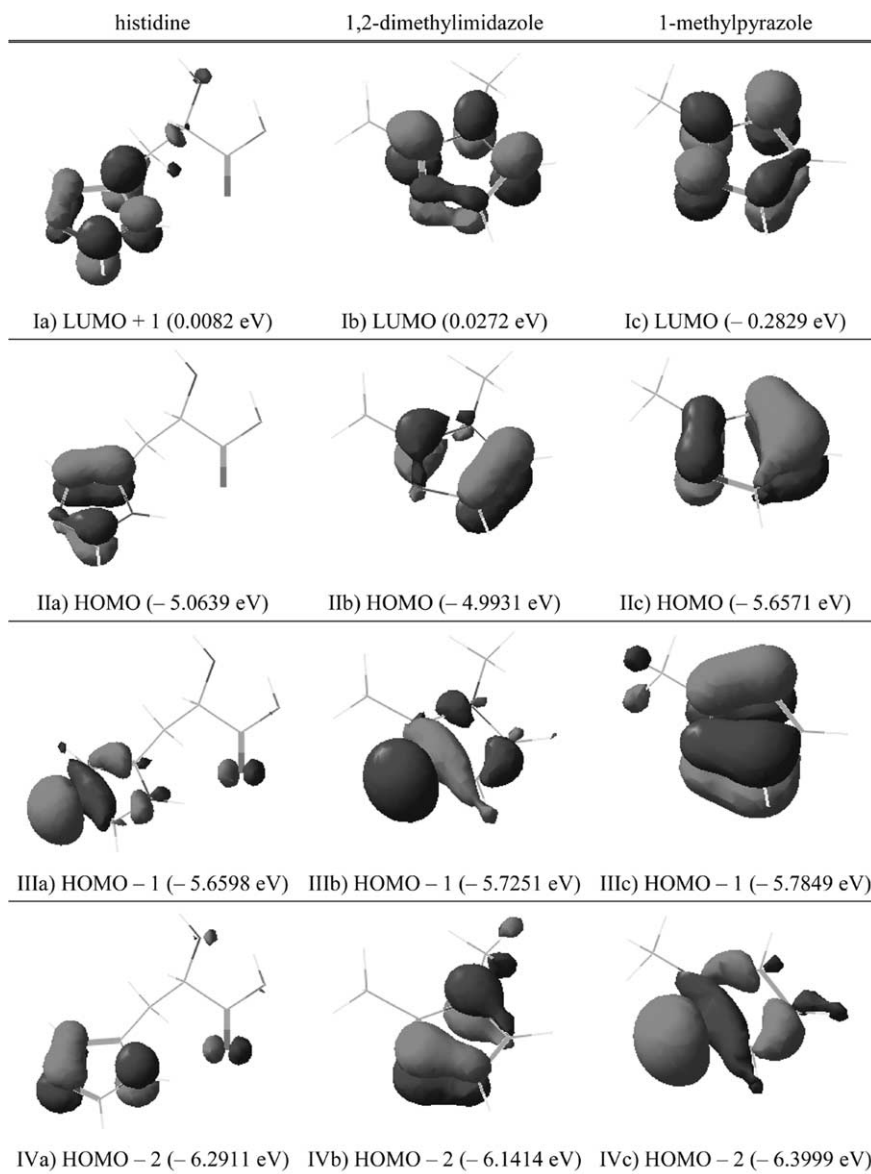
Fig. 2. Contour plots of the frontier orbitals of histidine, 1,2-dimethylimidazole and 1-methylpyrazole.

starting from bis(1-methylimidazol-2-yl)methane (Scheme 1), which had been prepared according to the literature [10]. Very recently, we noticed that parallel to our work van Koten and coworkers [11] have started research on the same compound.

By analogy to the preparation of 4,4-dimethyl-1,1-bis(1-methylimidazol-2-yl)pentan-3-one [10], 3,3-bis(1-methylimidazol-2-yl)methane is deprotonated with *n*BuLi at the bridging carbon atom. Subsequently, it reacts with methyl bromoacetate to give methyl 3,3-bis(1-methylimidazol-2-yl)propionate (bmipme, **1**) in high yields. The ester group of **1** is clearly visible in the IR spectra (1712 [CH_2Cl_2] and 1724 [KBr] cm^{-1}). The formation of **1** is easily detected by NMR. The signal of the proton at the bridging carbon atom is split into a triplet ($\delta = 5.00$ ppm, $^3J_{H,H} = 7.62$ Hz), and the protons

of the CH_2 group show a doublet ($\delta = 3.32$ ppm, $^3J_{H,H} = 7.62$ Hz). Furthermore, the presence of the ester group is indicated by resonances at 51.9 (OCH_3) and 171.7 ppm (CO_2R) in the ^{13}C NMR spectrum. Crystals suitable for single crystal X-ray structure determination were obtained from a solution in THF. In the molecular structure the 1-methylimidazolyl groups are slightly distorted against each other (Fig. 3). All bond lengths and angles are as expected.

Bmipme is saponified with aqueous NaOH to bis-3,3-(1-methylimidazol-2-yl)propionate (bmip) in quantitative yield. The ligand was isolated either as its sodium salt (Na[bmip], **2a**) or as its hydrochloride (Hbmip · 2HCl, **2b**), due to its high solubility in water. NMR spectra were recorded in D_2O or D_2O/acetone-d$_6$. In the ^{13}C NMR spectrum of **2a** the carboxylate group
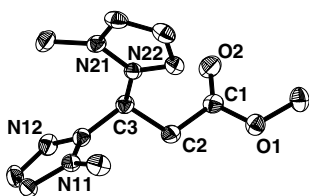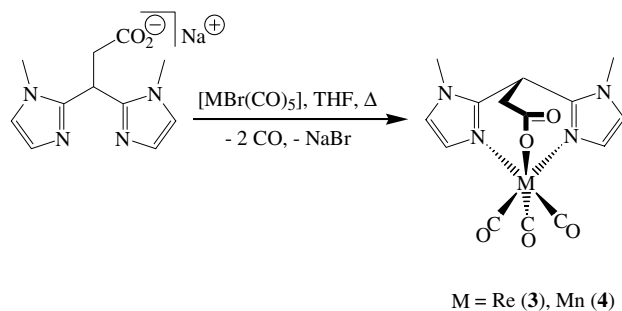
Fig. 3. Molecular structure of bmipme (**1**); thermal ellipsoids are drawn at a 50% probability level.

shows a resonance at 179.0 ppm. For **2b** this signal appears at 172.3 ppm. In contrast to the ^{1}H NMR spectra of **1**, **2a** and the complexes described below, the ^{1}H NMR spectrum of **2b** does not show two well separated doublets for the imidazolyl protons, but a multiplet.

2.3. Syntheses of the complexes [M(bmip)(CO)₃] (M = Re, Mn)

Since the binding properties of bmip and other known tripod ligands such as bpza, bdmpza, Tp and Tp^{Me_2} are best compared by IR spectroscopy and single crystal X-ray diffraction, we prepared manganese and rhenium tricarbonyl complexes of the new ligand. Complexes were synthesised by analogy to [M(bpza)(CO)₃] and [M(bdmpza)(CO)₃], starting from **2a** and the pentacarbonyl complexes [MnBr(CO)₅] and [ReBr(CO)₅] (Scheme 2) [12]. The progress of the reactions was monitored by IR spectroscopy. During the reactions CO evolution was observed. NaBr was removed from the products by washing with degassed water. Unlike the above-mentioned complexes with bis(pyrazol-1-yl)acetato ligands, **3** and **4** are soluble in methanol, but not in THF. Both complexes are as solids rather stable under aerobic conditions. Only **4** tends to decompose, when kept in solution. The two imidazolyl groups in the complexes are chemically equivalent, showing only one set of signals in the NMR spectra. The ^{1}H NMR signals of **4** are broad. The ^{13}C NMR spectra of both complexes exhibit two signals for the carbonyl ligands at a ratio of 2:1 (**3**: $\delta = 197.8$ and 198.0 ppm, **4**:

$\delta = 220.7$ and 225.3 ppm). The carboxylate group shows resonances at 171.3 ppm (**3**) or at 172.9 ppm (**4**).

Crystals suitable for X-ray determination of [Re-(bmip)(CO)₃] (**3**) and [Mn(bmip)(CO)₃] (**4**) were obtained from solutions in methanol/water (Figs. 4 and 5). Selected bond distances and angles are summarised in Tables 1 and 2.

In both complexes the bond distances between the carboxylate carbon atom and the adjacent carbon atom (C(3)–C(2)) and between the carboxylate carbon atom and the carboxylate oxygen atom (C(3)–O(1)) are slightly shorter than the analogous bonds in [Mn(bdmpza)(CO)₃], [Re(bdmpza)(CO)₃] and [Re-(bpza)(CO)₃] [12]. In **3** and **4** these bonds are less strained, because they are involved in the formation of a 7-membered ring instead of a 6-membered ring as in the aforementioned complexes. Furthermore, the diminished strain results in bond angles around the metal ion, which are generally closer to an ideal octahedron than in tricarbonyl complexes with bpza or bdmpza as ligands [12]. A second reason for this might be the low steric demand of the imidazolyl groups. The metal-carbonyl distances are in good agreement with those reported previously for [Mn(bdmpza)(CO)₃], [Re(bdmpza)(CO)₃] and [Re(bpza)(CO)₃] (Table 3) [12]. Accordingly, in both complexes **3** and **4** the metal-carbonyl distances M–C(31) and M–C(51) are longer than the metal-carbonyl distance M–C(41) *trans* to the carboxylate group. This
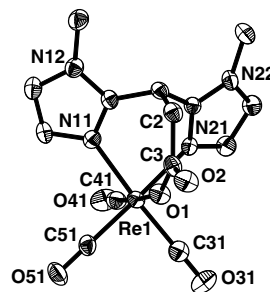
Fig. 4. Molecular structure of [Re(bmip)(CO)₃] (**3**); thermal ellipsoids are drawn at a 50% probability level.

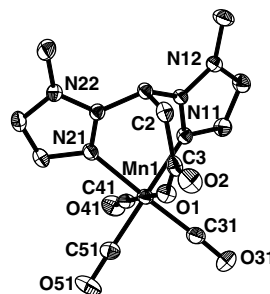Scheme 2. Synthesis of the complexes [M(bmip)(CO)₃] (M = Re, Mn) (**3**, **4**).

Fig. 5. Molecular structure of [Mn(bmip)(CO)₃] (**4**); thermal ellipsoids are drawn at a 50% probability level.

Table 1
Selected bond distances of the complexes **3** and **4**

Bond distance (Å)	**3**	**4**
M–N(11)	2.186(4)	2.058(3)
M–N(21)	2.184(5)	2.056(3)
M–O(1)	2.166(4)	2.104(2)
M–C(31)	1.953(6)	1.836(4)
M–C(41)	1.899(6)	1.800(3)
M–C(51)	1.928(6)	1.833(3)
C(3)–O(1)	1.287(7)	1.279(4)
C(3)–O(2)	1.262(7)	1.257(4)
C(3)–C(2)	1.538(8)	1.536(5)

Table 2
Selected bond angles of the complexes **3** and **4**

Bond angle (°)	**3**	Bond angle (°)	**4**
N(11)–Re–N(21)	83.81(17)	N(11)–Mn–N(21)	86.06(11)
O(1)–Re–N(11)	84.21(15)	O(1)–Mn–N(11)	87.29(10)
O(1)–Re–N(21)	83.13(18)	O(1)–Mn–N(21)	86.41(11)
O(1)–Re–C(41)	176.3(2)	O(1)–Mn–C(41)	178.16(12)
N(11)–Re–C(31)	175.7(2)	N(21)–Mn–C(31)	177.00(13)
N(21)–Re–C(51)	178.3(2)	N(11)–Mn–C(51)	178.58(13)
C(31)–Re–C(41)	89.4(2)	C(31)–Mn–C(41)	88.82(15)
C(51)–Re–C(41)	86.9(3)	C(51)–Mn–C(41)	86.78(15)
C(31)–Re–C(51)	88.5(3)	C(31)–Mn–C(51)	88.01(15)

is due to the *trans* influence of the two imidazolyl π acceptor groups onto the *trans* metal-carbonyl bonds.

The IR spectra of **3** and **4** are similar to those of "piano stool" complexes. Two strong signals A_1 and E are observed, of which E is split into two absorptions. As expected, the manganese CO signals are found at slightly higher wavenumbers than those of the rhenium complex. The IR spectra of the complexes **3** and **4** show carbonyl vibration frequencies lower compared to those of the corresponding bis(pyrazol-1-yl)acetato complexes

(Table 4) [12]. These data suggest that pyrazol-1-yl and 1-methylimidazol-2-yl groups may have almost the same donor strength, but that the 1-methylimidazol-2-yl group is a weaker π acceptor. This observation is in good agreement with the DFT calculations.

3. Conclusion

The new monoanionic, facially coordinating tripod ligand bmip was studied. As first examples of its coordination properties the tricarbonyl complexes [Re(bmip)(CO)$_3$] and [Mn(bmip)(CO)$_3$] were prepared and characterised by single crystal X-ray crystallography. The results show that bmip and similar ligands might be versatile ligands in different fields of coordination and bioinorganic chemistry. They may be applied in the synthesis of structural and possibly functional iron, zinc and ruthenium model complexes for enzymes containing the 2-histidine-1-carboxylate motif. Furthermore, the complexes **3** and **4** suggest, that bmip might be a suitable ligand in future rhenium and technetium complexes for radiopharmaceutical applications [13–15].

4. Experimental

4.1. General

All operations were carried out under nitrogen atmosphere by using conventional Schlenk techniques. Solvents were distilled from appropriate drying agents and degassed before use. The yields refer to analytically pure compounds and were not optimised.

Table 3
Metal-carbonyl distances of the complexes [ML(CO)$_3$] (M = Re, Mn; L = bmip, bpza, bdmpza)

Ligand	bmip		bpza [12]		bdmpza [12]	
Bond distance (Å)	*trans* to N-donor	*trans* to CO_2^-	*trans* to N-donor	*trans* to CO_2^-	*trans* to N-donor	*trans* to CO_2^-
d(Re–CO)	1.953(6)	1.899(6)	1.952(9)	1.930(10)	1.956(14)	1.943(12)
	1.928(6)		1.947(8)		1.973(13)	
d(Mn–CO)	1.836(3)	1.800(3)	–	–	1.819(4)	1.804(4)
	1.833(4)		–		1.816(4)	

Table 4
Selected IR signals (cm^{-1}) of [MnL(CO)$_3$] and [ReL(CO)$_3$] (M = Re, Mn; L = bmip, bpza, bdmpza)

Ligand L	bmip	bpza	bdmpza
ν(CO) (CH$_3$OH) [ReL(CO)$_3$]	2023, 1914, 1896	–	2030, 1926, 1908
ν(CO) (KBr) [ReL(CO)$_3$]	2018, 1898, 1867	2028, 1922, 1906, 1895 [12]	2023, 1915, 1903, 1883 [12]
ν(CO) (CH$_3$OH) [MnL(CO)$_3$]	2035, 1936, 1918	2046, 1955, 1937	2041, 1949, 1927
ν(CO) (KBr) [MnL(CO)$_3$]	2027, 1922, 1895	2039, 1952, 1943, 1927, 1916 [12]	2036, 1924 [12]

- IR: Biorad FTS 60, CaF_2 cuvets (0.5 mm).
- ^1H NMR and ^{13}C NMR: Bruker AC 250 or Varian Inova 400, δ values relative to TMS or the deuterated solvent.
- Mass spectra were recorded on a modified Finnigan MAT 312 using either EI or FAB technique with 3-nitrobenzyl alcohol as matrix.
- Elemental analyses: Heraeus CHN-O-Rapid.
- A modified Siemens P4 diffractometer was used for X-ray structure determination.
- Chemicals were used as purchased without further purification. Bis(1-methylimidazol-2-yl)methane, [ReBr(CO)$_5$] and [MnBr(CO)$_5$] were synthesised according to the literature [10,16,17].

4.2. Ligand synthesis

Bmipme (1): A solution of bis(1-methylimidazol-2-yl)methane (10.0 g, 56.7 mmol) in THF (abs., 300 ml) was cooled to $-80\ ^\circ C$. After addition of *n*BuLi (27.8 ml, 2.2 M/hexane, 61.2 mmol) the mixture was allowed to warm to $-40\ ^\circ C$ over a period of 2 h. After addition of methyl 2-bromoacetate (5.60 ml, 61.3 mmol) the mixture was allowed to warm to room temperature. The solvent was removed in vacuo, and the residue was dissolved in H_2O and CH_2Cl_2. The organic phase was separated, and the aqueous phase was extracted with CH_2Cl_2 (4×50 ml). The combined organic layers were dried (Na_2SO_4), and the solvent was removed in vacuo. The crude product was recrystallised from THF. Crystals suitable for X-ray structure determination were obtained from a solution in THF.

Yield: 11.3 g (45.5 mmol, 80%). m.p. 68–70 °C. ^1H NMR (250 MHz, CDCl$_3$): $\delta = 3.32$ (d, $^3J_{H,H} = 7.62$ Hz, 2H, CH$_2$), 3.49 (s, 6H, NCH$_3$), 3.67 (s, 3H, OCH$_3$), 5.00 (t, $^3J_{H,H} = 7.62$ Hz, 1H, CH$_{bridge}$), 6.77 (d, $^3J_{H,H} = 1.23$ Hz, 2H, CH$_{imid}$), 6.93 (d, $^3J_{H,H} = 1.23$ Hz, 2H, CH$_{imid}$). ^{13}C NMR (62.9 MHz, CDCl$_3$): $\delta = 32.8$ (NCH$_3$), 34.6 (CH$_{bridge}$), 36.2 (CH$_2$), 51.9 (OCH$_3$), 122.0, 127.3 ($2 \times C_{imid}$), 145.3 (C=N), 171.7 (CO$_2$R). EI MS (70 eV, 100 °C): m/z (%) = 248 (59) [M$^+$], 217 (42) [M$^+$ − MeOH], 189 (100) [M$^+$ − MeOH − CO]. IR (KBr): $\nu_{max} = 1724$ s (CO$_2$R) cm^{-1}; IR (CH$_2$Cl$_2$): $\nu_{max} = 1712$ s (CO$_2$R) cm^{-1}. Elemental analysis (C$_{12}$H$_{16}$N$_4$O$_2$, M = 248.28 g mol^{-1}): Calc: C 58.05, H 6.50, N 22.57. Found: C 57.63, H 6.18, N 22.19.

Na[bmip] (2a): Bmipme (8.70 g, 35.0 mmol) was dissolved in THF (200 ml), and NaOH (1.33 g, 33.3 mmol, aqueous solution) was added. The mixture was heated under reflux for 3 h. After this period the solvent was removed in vacuo. The residue was dissolved in water and washed with CH$_2$Cl$_2$ (5×20 ml) to remove remainders of the educt. The aqueous phase was dried in vacuo. The residue was recrystallised from MeOH/Et$_2$O to yield a white solid.

Yield: 7.63 mg (29.8 mmol, 85%). m.p. >260 °C (dec.). ^1H NMR (250 MHz, D$_2$O): 2.91 (d, $^3J_{H,H} = 7.62$ Hz, 2H, CH$_2$), 3.43 (s, 6H, NCH$_3$), 4.71 (t, $^3J_{H,H} = 7.62$ Hz, 1H, CH$_{bridge}$), 6.81 (d, $^3J_{H,H} = 0.9$ Hz, 2H, H$_{imid}$), 6.95 (s, br, 2H, H$_{imid}$). ^{13}C NMR (62.9 MHz, D$_2$O/5% acetone-d$_6$): 32.7 (NCH$_3$), 33.4 (CH$_{bridge}$), 39.8 (CH$_2$), 122.9, 126.3 ($2 \times C_{imid}$), 147.1 (C=N), 179.0 (CO$_2^-$). EI MS (70 eV, 300 °C): m/z (%) = 279 (34) [Na[bmip] + Na$^+$], 188 (100) [bmip − CO$_2$H]. IR (MeOH): $\nu_{max} = 1591$ m (ν_{as}-CO$_2^-$) cm^{-1}. Elemental analysis (C$_{11}$H$_{13}$N$_4$NaO$_2 \times$ H$_2$O, M = 274.25 g mol^{-1}): Calc: C 48.17, H 5.51, N 20.43. Found: C 48.09, H 5.58, N 19.67.

Hbmip · 2HCl (2b): Bmipme (6.75 g, 27.2 mmol) was dissolved in THF (200 ml), and NaOH (1.02 eq., aqueous solution) was added. The mixture was heated under reflux for 3 h. After this period the solution was neutralised with conc. HCl. The solvent was removed in vacuo. The residue was dissolved in conc. HCl and the insoluble salts were filtered off. The solvent was removed, and the residue was recrystallised from MeOH/THF to yield a white solid.

Yield 7.42 g (24.2 mmol, 89 %). m.p. >230 °C (dec.). ^1H NMR (250 MHz, D$_2$O): 3.50 (d, $^3J_{H,H} = 7.32$ Hz, 2H, CH$_2$), 3.85 (s, 6H, NCH$_3$), 5.59 (t, $^3J_{H,H} = 7.30$ Hz, 1H, CH$_{bridge}$), 7.49 (m, 4H, H$_{imid}$). ^{13}C NMR (62.9 MHz, D$_2$O/5% acetone-d$_6$): 29.7 (CH$_{bridge}$), 34.9 (CH$_2$), 35.2 (NCH$_3$), 120.4, 125.6 ($2 \times C_{imid}$), 140.2 (C=N), 172.3 (CO$_2$H). EI MS (70 eV, 170 °C): m/z (%) = 234 (36) [Hbmip], 190 (100) [Hbmip − CO$_2$]. IR (MeOH): $\nu_{max} = 1728$ s (ν_{as}-CO$_2$H) cm^{-1}. IR (KBr): $\nu_{max} = 1699$ br (ν_{as}-CO$_2$H) cm^{-1}. Elemental analysis (C$_{11}$H$_{16}$Cl$_2$N$_4$O$_2$, M = 307.18): Calc: C 43.01, H 5.25, N 18.24. Found: C 42.64, H 5.19, N 17.77.

4.3. Syntheses of the complexes [M(bmip)(CO)$_3$] (M = Re, Mn)

[Re(bmip)(CO)$_3$] (3): Na[bmip] (139 mg, 0.542 mmol) and [ReBr(CO)$_5$] (200 mg, 0.492 mmol) are dissolved in THF (abs., 30 ml) and heated under reflux. The progress of the reaction is monitored by IR spectroscopy. After completion of the reaction the solvent is removed in vacuo. The white residue is washed with water (3×10 ml), THF (3×10 ml) and Et$_2$O (1×10 ml) and dried in vacuo. Crystals suitable for a single crystal X-ray diffraction experiment were obtained from a solution in MeOH/H$_2$O.

Yield: 178 mg (0.353 mmol, 72%). m.p. >315 °C (dec.). ^1H NMR (400 MHz, DMSO-d$_6$): $\delta = 2.80$ (d, $^3J_{H,H} = 3.92$ Hz, 2H, CH$_2$), 3.81 (s, 6H, NCH$_3$), 4.71 (t, $^3J_{H,H} = 3.88$ Hz, 1H, CH$_{bridge}$), 7.29 (d, $^3J_{H,H} = 1.56$ Hz, 2H, CH$_{imid}$), 7.39 (d, $^3J_{H,H} = 1.56$ Hz, 2H, CH$_{imid}$). ^{13}C NMR (100.5 MHz, DMSO-d$_6$): $\delta = 29.4$ (CH$_{bridge}$), 33.8 (NCH$_3$), 42.3 (CH$_2$), 123.2, 129.5 ($2 \times C_{imid}$), 146.0 (C=N), 171.3 (CO$_2^-$), 197.8 (CO), 198.0

($2 \times CO$). FAB MS (NBOH matrix): m/z (%) = 505 (67) [MH^+]. IR (MeOH): v_{max} = 2024 s (CO), 1914 s (CO), 1897 s (CO), 1588 m (v_{as}-CO_2^-) cm^{-1}. IR (KBr): v_{max} = 2018 s (CO), 1898 s (CO), 1867 s (CO), 1589 m (v_{as}-CO_2^-) cm^{-1}. Elemental analysis ($C_{14}H_{13}N_4O_5Re \times$ 2 CH_3OH, M = 567.57 g mol^{-1}): Calc: C 33.92, H 3.56, N 9.89. Found: C 33.70, H 3.77, N 10.10.

[Mn(bmip)(CO)$_3$] (4): Na[bmip] (1.03 g, 4.00 mmol) and [MnBr(CO)$_5$] (1.00 g, 3.64 mmol) are dissolved in THF (abs., 50 ml) and heated under reflux. The progress of the reaction is monitored by IR spectroscopy. After completion of the reaction the solvent is removed in vacuo. The crude product is either purified by column chromatography (neutral alumina, gradient from pure CH_2Cl_2 to CH_2Cl_2:MeOH 1:1 v/v) or washed with water (3×10 ml), THF (3×10 ml) and Et$_2$O (1×10 ml) and dried in vacuo to give a yellow powder. Crystals suitable for X-ray structure determination were obtained from a solution in methanol/water under argon.

Yield: 1.19 g (3.22 mmol, 88%). m.p. >219 °C (dec.). ^{1}H NMR (400 MHz, DMSO-d$_6$): δ = 3.17 (s, br, 2H, CH$_2$), 3.78 (s, br, 6H, NCH$_3$), 4.57 (s, br, 1H, CH$_{bridge}$),

7.36 (s, br, 4H, CH$_{imid}$). ^{13}C NMR (100.5 MHz, DMSO-d$_6$): 28.7 (CH$_{bridge}$), 33.6 (NCH$_3$), 48.6 (CH$_2$), 122.6, 129.2 ($2 \times C_{imid}$), 146.3 (C=N), 172.9 (CO$_2^-$), 220.7 ($2 \times CO$), 225.3 (CO). FAB MS (NBOH): m/z (%) = 373 (32) [MH^+], 244 (83) [M^+ – 3 CO – CO_2]. IR (MeOH): v_{max} = 2035 s (CO), 1936 s (CO), 1919 s (CO), 1587 m (v_{as}-CO_2^-) cm^{-1}. IR (KBr): v_{max} = 2027 s (CO), 1922 s (CO), 1895 s (CO), 1584 m (v_{as}-CO_2^-) cm^{-1}. Elemental analysis ($C_{14}H_{13}MnN_4O_5 \times 3$ H_2O, M = 426.27 g mol^{-1}): Calc: C 39.45, H 4.49, N 13.14. Found: C 40.06, H 4.55, N 13.37.

4.4. Calculations

DFT-calculations and full geometry optimisations were carried out by using Jaguar 5.5.0.16 [18] running on Linux 2.4.20–28.7smp on six Athlon MP 2400+ dual-processor workstations (Beowulf-cluster) parallelised with MPICH 1.2.4. MM2 optimised structures were used as starting geometries. Complete geometry optimisations were carried out on the implemented

Table 5
Details of the structure determination of compounds bmipme (**1**), [Re(bmip)(CO)$_3$] (**3**) and [Mn(bmip)(CO)$_3$] (**4**)

	bmipme (**1**)	[Re(bmip)(CO)$_3$] (**3**)	[Mn(bmip)(CO)$_3$] (**4**)
Empirical formula	$C_{12}H_{16}N_4O_2$	$C_{14}H_{13}N_4O_5Re \times 2$ CH_3OH	$C_{14}H_{13}MnN_4O_5 \times 3$ H_2O
Formula weight	248.29	567.57	426.27
Crystal colour/habit	Colourless block	Colourless block	Yellow block
Crystal system	Monoclinic	Orthorhombic	Monoclinic
Space group	$C2/c$	$P2_12_12_1$	$P2_1/n$
Unit cell dimensions			
a (Å)	16.541(5)	10.997(10)	11.656(6)
b (Å)	9.889(4)	11.437(7)	8.730(5)
c (Å)	16.286(7)	16.376(10)	18.257(9)
α (°)	90	90	90
β (°)	111.219(19)	90	106.88(3)
γ (°)	90	90	90
V (Å^3)	2483.2(16)	2060(3)	1777.9(15)
θ (°)	2.45–27.00	2.17–26.99	2.33–26.99
h	−21 to 21	−14 to 11	0–14
k	−12 to 12	−14 to 14	−11 to 0
l	−20 to 19	−20 to 20	−22 to 22
Z	8	4	4
μ (Mo Kα) (mm^{-1})	0.094	5.943	0.794
Crystal size	$0.5 \times 0.5 \times 0.3$	$0.5 \times 0.4 \times 0.3$	$0.5 \times 0.4 \times 0.3$
T (K)	188(2)	188(2)	188(2)
Reflections collected	4949	4467	4053
Independent reflections	2724	4007	3865
Obs. refl. (>$2\sigma I$)	2234	3846	3130
R_{int}	0.0437	0.0242	0.0229
Parameter	163	260	262
Weight parameter a	0.0637	0.0342	0.0764
Weight parameter b	1.2810	0.8523	2.7941
R_1 (obs.)	0.0462	0.0267	0.0523
R_1 (overall)	0.0582	0.0289	0.0673
wR_2 (obs.)	0.1182	0.0644	0.1392
wR_2 (overall)	0.1275	0.0655	0.1481
Difference in peak/hole (e Å^3)	0.311/−0.377	0.790/−1.081	0.868/−1.050

BP86/LACVP∗ basis set. Orbital plots [19] were obtained using Maestro 6.5006, the graphical interface of Jaguar [18].

4.5. X-ray structure determinations

Single crystals of **1**, **3** and **4** were mounted with Paratone-N on glass fibres. A modified Siemens P4 diffractometer was used for data collection (graphite monochromator, Mo Kα radiation, $\lambda = 0.71073$ Å, scan rate 4–30° min^{-1} in ω). A ψ-scan absorption correction was applied to the datasets of **3** and **4**. The structures were solved and refined with full-matrix least-squares against F^2 by using the SHELX-97 program package [20]. A weighting scheme was applied in the last steps of the refinement with $w = 1/[\sigma^2(F_o^2) + (aP)^2 + bP]$ and $P = [2F_c^2 + \text{Max}(F_o^2, 0)]/3$. In compound **3** two molecules methanol co-crystallised per asymmetric unit. One of the methanol molecules forms a hydrogen bond to the oxygen atom O(2) of the ligand with d(O(2)–O(61)) = 2.756 Å. A second hydrogen bond exists between the two methanol molecules with d(O(61)–O(71)) = 2.801 Å. In compound **4** three molecules H_2O co-crystallise per asymmetric unit. Water molecules of different asymmetric units form hydrogen bonds to the oxygen atom O(2) of the ligand [d(O(2)–O(61)) = 2.796 Å, d(O(2)–O(71)) = 2.887 Å] and among themselves [d(O(61)–O(71)) = 2.340 Å, d(O(71)–O(81)) = 2.780 Å]. The O–H hydrogen atoms in structure **3** and **4** were found, but restraints had to be applied for these during the refinement. All the other hydrogen atoms were included in their calculated positions and refined in a riding model. Details and parameters of the measurements are summarised in Table 5. The structure pictures were prepared with the program Diamond 2.1e [21]. Crystallographic data (excluding structure factors) for the structures reported in this paper have been deposited with the Cambridge Crystallographic Data Centre as supplementary publication No. CCDC-255157 (bmipme, **1**), CCDC-255158 ([Re(bmip)(CO)$_3$], **3**) and CCDC-255159 ([Mn(bmip)(CO)$_3$], **4**) These data can be obtained free of charge at www.ccdc.cam.ac.uk/conts/retrieving.html or from the Cambridge Crystallographic Data Centre, 12 Union Road, Cambridge CB2 1EZ, UK [Fax: (internat.) +44-1223-336-033; e-mail: deposit@ccdc.cam.ac.uk].

References

[1] S. Trofimenko, Scorpionates – The Coordination Chemistry of Polypyrazolylborate LigaImperial College Press, Imperial College Press, London UK, 1999, and references cited therein.

[2] A. Otero, J. Fernández-Baeza, A. Antiñolo, J. Tejeda, A. Lara-Sánchez, Dalton Trans. (2004) 1499, and references cited therein.

[3] M. Costas, M.P. Mehn, M.P. Jensen, L. Que Jr., Chem. Rev. 104 (2004) 939, and references cited therein.

[4] G. Parkin, Chem. Rev. 104 (2004) 699, and references cited therein.

[5] (a) M. Joseph, T. Leigh, M.L. Swain, Synthesis (1977) 459;
(b) B. Gimeno, A. Sancho, L. Soto, J.-P. Legros, Acta Cryst. C 52 (1996) 1226;
(c) B. Gimeno, L. Soto, A. Sancho, F. Dahan, J.-P. Legros, Acta Cryst. C 48 (1992) 1671.

[6] (a) Y. Akhriff, J. Server-Carrió, A. Sancho, J. García-Lozano, E. Escrivá, J.V. Folgado, L. Soto, Inorg. Chem. 38 (1999) 1174;
(b) Y. Akhriff, J. Server-Carrió, A. Sancho, J. García-Lozano, E. Escrivá, L. Soto, Inorg. Chem. 40 (2001) 6832;
(c) A. Sancho, B. Gimeno, J.-M. Amigó, L.-E. Ochando, T. Debaerdemaeker, J.-V. Folgado, L. Soto, Inorg. Chim. Acta 248 (1996) 153;
(d) H. Núsimnez, E. Escrivà, J. Server-Carrió, A. Sancho, J. García-Lozano, L. Soto, Inorg. Chim. Acta 324 (2001) 117.

[7] (a) Z. Likó, H. Süli-Vargha, Tetrahedron Lett. 34 (1993) 1673;
(b) K. Ősz, K. Várnagy, H. Süli-Vargha, D. Sanna, G. Micera, I. Sóvágó, Dalton Trans. (2003) 2009;
(c) K. Várnagy, I. Sóvágó, K. Ágoston, Z. Likó, H. Süli-Vargha, D. Sanna, G. Micera, J. Chem. Soc. Dalton Trans. (1994) 2939;
(d) K. Ősz, K. Várnagy, H. Süli-Vargha, A. Csámpay, D. Sanna, G. Micera, I. Sóvágó, J. Inorg. Biochem. 98 (2004) 24;
(e) K. Várnagy, I. Sóvágó, W. Goll, H. Süli-Vargha, G. Micera, D. Sanna, Inorg. Chim. Acta 283 (1998) 233.

[8] R.H. Holm, P. Kennepohl, E.I. Solomon, Chem. Rev. 96 (1996) 2239.

[9] The LUMO of histidine extends over the carboxylate group of the amino acid and hence is not shown in the diagram and has been omitted in the comparison. Therefore, the LUMO + 1 of histidine is compared to the LUMOs of 1-methylpyrazole and 1,2-dimethylimidazole.

[10] N. Braussaud, T. Rüther, K.J. Cavell, B.W. Skelton, A.H. White, Synthesis (2001) 626.

[11] P.C.A. Bruijnincx, J.P. den Breejen, M. Lutz, A.L. Spek, B.M. Weckhuysen, G. van Koten, R.J.M. Klein Gebbink, poster presentation P-40 at the EUROBIC 7, Garmisch-Partenkirchen 2004.

[12] N. Burzlaff, I. Hegelmann, B. Weibert, J. Organomet. Chem. 626 (2001) 16.

[13] J. Bernard, K. Ortner, B. Spingler, H.-J. Pietzsch, R. Alberto, Inorg. Chem. 42 (2003) 1014.

[14] N. Metzler-Nolte, Angew. Chem., Int. Ed. Engl. 40 (2001) 1040.

[15] F. Le Bideau, M. Salmain, S. Top, G. Jaouen, Chem. Eur. J. 7 (2001) 2289.

[16] E.W. Abel, G. Wilkinson, J. Chem. Soc. (1959) 1501.

[17] D. Vitali, F. Calderazzo, Gazz. Chim. Ital. 102 (1972) 587.

[18] Jaguar 5.5, Schrödinger, LLC, Portland, Oregon, 2003.

[19] R. Stowasser, R. Hoffmann, J. Am. Chem. Soc. 121 (1999) 3414.

[20] G.M. Sheldrick, SHELX-97, Programs for Crystal Structure Analysis, University of Göttingen, Göttingen, Germany, 1997.

[21] K. Brandenburg, M. Berndt, Diamond – Visual Crystal Structure Information System, Crystal Impact GbR, Bonn, Germany, 1999; for a Software review see: W.T. Pennington, J. Appl. Crystallogr. 32 (1999) 1028.